THE EFFECTS OF NONLINEAR SPECTRAL MIXTURE ANALYSIS ON END-MEMBER OPTIMIZATION IN ANALYSIS OF HYPERSPECTRAL IMAGE DATA. Guoqi He and John F. Mustard. Department of Geological Science, Box 1846, Brown University, Providence RI, 02912. (Guoqi_He@brown.edu)

Hapke's [1,2] comprehensive work on the solution of the radiative transfer problem for a particulate medium has been applied in a number of studies [3,4,5] to derive first-order analytic expressions relating reflectance, albedo, and single-scattering albedo for the extraction of abundance of materials from remotely sensed data. Linear spectral mixture analysis (SMA) [3 through 12] has been widely used in the analysis of laboratory [3,4,5,6] and field data[7,8] (terrestrial and extraterrestrial spectroscopic, multispectral, and hyperspectral) with great success. Although it is widely acknowledged that radiative transfer solutions provide more accurate abundance estimates for intimate mixtures, linear SMA is primarily used in imaging applications. Differences (>10%) in physical abundance estimates between linear and nonlinear solutions is lager than either the instrument measurement errors (1-2 DN for 8-bit encoding) or the accuracy (<10%) of the radiative transfer theory[2]. This discrepancy is largely due to the fact mixing is largely nonlinear at the scale of observation, and there is only a limited number of end-members the mixing equation can accommodate at a time.

In this analysis, we apply nonlinear mixture analysis to hyperspectral data and focus on 3 key issues: spectral end-member characterization, subpixel component abundance quantification, and error magnitude and distribution for band residuals and total RMS errors. The hyperspectral data was collected by HYperspectral Digital Imagery Collection Experiment (HYDICE) instrument. Nonlinear analysis provides a different view over a pure linear approach with respect to each of the three major factors.

HYDICE is a pushbroom system patterned into a 210 (channel) by 320 (pixel) array of detector elements with dynamic range of 12 bits. It has an IFOV of 0.5milliradian. Data collected at a altitude of 2,000m (1m GSD) and 6,000m(3m GSD) over a semi-arid region of Arizona were calibrated to reflectance using a series of calibration panels in the scene. The reflectance data for both 1 and 3 meter resolutions were transformed to SSA using the algorithms of [3].

Spectral End-member Characterization: The criteria for end-member selection are to balance the minimization of RMS error, to derive physically meaningful end-member spectra (representative of physically realistic materials) and to produce a well bounded end-member fraction map. Two different methods are used to study the difference between the linear and nonlinear approaches. One is to use 3 end-members to simulated a "minimum" end-members solution. The other uses 6 for the "maximum" situation. We find fundamentally different sets of end-members for the reflectance vs. SSA data sets in order to reach the optimum solution (Figures 1a and b). This is especially true when the number of end-members input into SMA is more than three and one less than the maximum. In this case, one needs to have more end members in the higher albedo range than in the lower albedo range for the linear approach, while more low albedo relative to high albedo end-member are required for the nonlinear situation. The differences between the linear and nonlinear data sets are coupled to the SSA transform. This transform reduces spectral contrast in higher albedo materials and increases spectral contrast in lower albedo material (relative to reflectance). Spectral contrast here refers not only to absorption band strength in a single material, but also to the contrast between materials and overall continuum. As a consequence, a different set of end-members is required to optimize the mixing solution for the SSA data relative to the reflectance data.

Subpixel Abundance Quantification: Linear SMA gives an adequate representation of the spatial relationship and physical abundance of the components if the mixing systematics are linear. However, in many planetary situations, intimate mixing is the norm and nonlinear mixing should be employed for more accurate abundance determination. For the desert soils in this region of Arizona, we expect the end-members to be intimately mixed at the 1-3 meter scale. To evaluate the difference between the linear and nonlinear mixing on hyperspectral data, we present the results of the 3-component mixing in Figure 2. The absolute differences in abundance can be as much as 30%. Detailed analysis of this data cloud for each individual component (Figure 3) reveals two distinctively different relationships, one being linear, and the other curve-linear. Each of the trends maps out the spatial relationship of the scene for the given end-member. The other major difference between these two different approaches is described by the amount of super positive and negative points in the scene. The nonlinear model is often much better constrained and has less super positive and negative data numbers. Along with the lab studies [3,4], we believe the nonlinear model is a better model to use in light of the Hapke's photometric radiative transfer theory provided the data are calibrated to reflectance, and the assumptions in SSA transform are met [2,3,4].

Error Magnitude and Distribution: The average RMS error for the nonlinear SMA is generally one half the average RMS of the linear SMA solution, regardless the number of end-members used in the analysis. In addition, the average RMS error (less than 1%) for the nonlinear model is comparable with the instrumental error. Therefore, the selection of image end-members must be done carefully to avoid end-members that model the instrumental error. Spatially, the error map from nonlinear SMA shows a more random pattern than from the linear SMA. Exhaustive study of multiple image end-member combinations suggests that the end-member set from the least RMS error solution may produce

fractions that are not well connected to physical abundance. Equally important is that end-member selected from spectral libraries (Lab or field based) may not be comparable to the reflectance of image end-member in hyperspectral data set. Thus we believe that the best approach is to model the image data using image end-member, and that the image end-member be modeled with lab or field data subsequently.

Conclusions: Nonlinear model clearly provides advantage to the understanding of end-members and their application to SMA. It also enhances our ability to extract more realistic end-member fractions. RMS error from nonlinear model is approaching the instrument error. This is especially true for the well modeled background which is the majority of the scene.

References:

[1] Hapke, B. JGR 86, 3039-3054. [2] Hapke, B. *Theory of Reflectance and Emittance Spectroscopy*, Cambridge Press, 1993. [3] Mustard, J. F. and C. M. Pieters, JGR 94, 13619-13634, 1989. [4] Mustard, J. F. and C. M. Pieters, JGR 92, E617-E626, 1987. [5] Johnson, P. E., et al., JGR 88, 3357-3361, 1983. [6] Mustard, J. F., RSE 44, 1-25, 1993 . [7] Herzog, S. and J. F. Mustard, LPSC XXVII, 535-536, 1996. [8] Li, et al, LPSC XXVIII, this volume. [9] Li, et al, LPSC XXVIII, this volume. [10] Tompkins, S., et al., Optimization of End-members in Spectral Mixture Analysis, Ch4. Thesis, Brown University, 1997. [11] Sabol, D. E., et al., JGR 97, 2659-2672. [12] Adams, J. B., et al., in *Remote Geochemical Analysis: Elemental and Mineralogical Composition*, Cambridge Press, pp. 145-166, 1993.

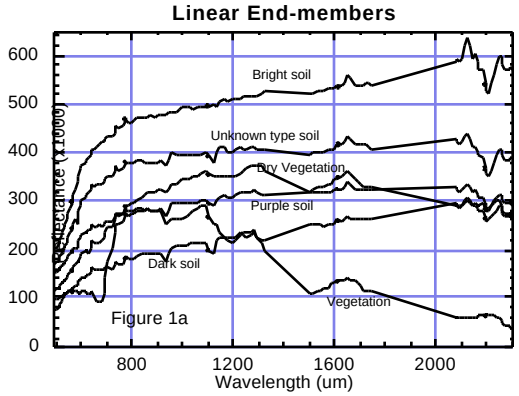

Figure 1a: Linear end-member selected from a 3-meter image scene. More higher albedo end-member can be accommodated in the SMA analysis.

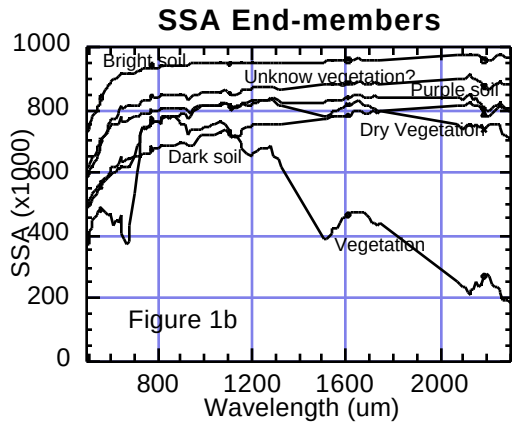

Figure 1b: Nonlinear end-member selected from the same scene with SSA transformation. More low albedo end-member can be accommodated in the SMA analysis.

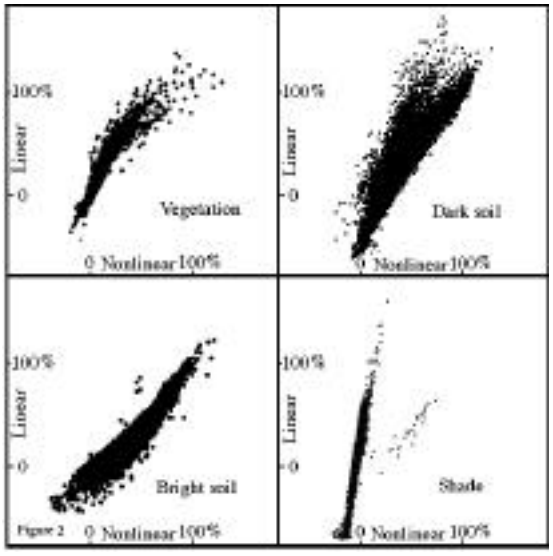

Figure 2: Scatter plots of linear vs., Nonlinear SMA analysis from 3 end-member shows different approach produces very different fraction results.

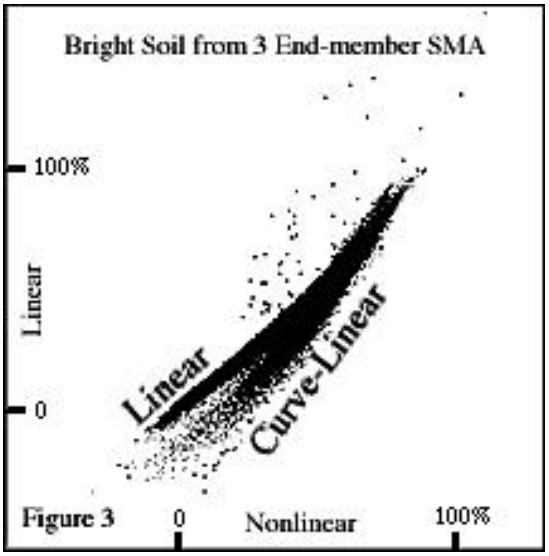

Figure 3: The expanded view of bright soil fraction from Figure 2 clearly shows both the linear and curve-linear partition of the fraction data cloud.